

Dynamic and static deuterium inventory in ASDEX Upgrade with tungsten first wall

V. Rohde, M. Mayer, V. Mertens, R. Neu, K. Sugiyama and the ASDEX Upgrade Team

Max-Planck-Institut für Plasmaphysik, EURATOM Association, D-85748 Garching, Germany

e-mail contact of main author: Volker.Rohde@ipp.mpg.de

Abstract. Deuterium retention in the divertor tokamak ASDEX Upgrade is studied by surface analysis and gas balances. Comparing C and W plasma facing components, the deuterium content of deposits at the divertor plates is dropped by a factor of 13. At the outer divertor significant implantation into the W coating is found. Deposition at remote areas is reduced by a factor of 14. Gas balances for ITER relevant high density H-mode discharges leads to an D retention averaged over a discharge of $8.2 \pm 3.3\%$ for W PFC and $23 \pm 7\%$ for C PFC. For W PFC's wall saturation is observed, i.e. only $1.5 \pm 3.5\%$ of the puffed gas is retained. Within the error bars all D outgases within 15 min.

1. Introduction

The first wall material of a future fusion reactor has to match different requirements. The material has to withstand thermal loads, the erosion rate must be low to allow ample operation time, the dilution of and the radiation in the core plasma must be tolerable and the storage of deuterium must be low. The present ITER design tries to match the different requirements using a mix of Be, W and carbon fibre composites (CFC) surfaces. An alternative to this material mix is a complete high Z wall. This option is tested in ASDEX Upgrade (AUG) with tungsten plasma facing components (PFC). A stepwise transition from carbon to tungsten coated carbon tiles was selected to minimize the effort and to study the material migration [1],[2].

Deuterium (D) in a fusion device is stored mainly by implantation in the bulk material, diffusion and trapping at natural or ion induced traps, co-deposits with eroded PFC as carbon and adsorption at the surface. Cleaning of implanted material is difficult as the D is bound inside the material, but for safety reasons a higher inventory is tolerable. In co-deposits D is chemical bound in layers on the surface. The D can be released by heating the surface or dust formation, for example by flaking of the layers. The co-depositions are the dominate safety risk, as in carbon devices they store most of the D. Absorption is done on the surface, the D is released within some hours.

In this paper we discuss two methods to measure the D retention in AUG. The first method is to measure the D content of the PFC. A set of new tiles was build in, exposed and post mortem analyzed by ion beam techniques [3]. The advantage of this method is the high sensitivity of the analysis, the problem is to cover all deposition areas. As the tiles are analyzed after the campaign, the result is a weighted average of all discharges. In FIG. 1 a cross section of AUG including the tiles, which were analyzed is shown. The other method is gas balance, which determines for each discharge the gas input and gas removal. The main problem of this technique is to reach a adequate accuracy. The positions of the gas input and pumping systems

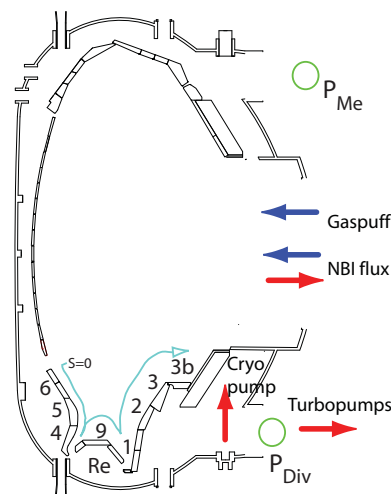


FIG. 1: Position of the tiles (1-9) and remote areas (Re) used for post mortem analysis. The pumps and gauges are also indicated.

taken into account is also indicated in *FIG. 1*.

2. Deposition on Plasma Facing Components

The main plasma wall interaction in AUG is located in the divertor. A set of divertor tiles, equipped with markers, which are analyzed before and after a campaign, allows to determine the deposition and erosion at the different positions [3]. The tiles were replaced after each campaign to study the stepwise transition to a full tungsten device, which allows to identify the primary carbon sources. Here we concentrate on the results of the 2002/03 campaign, which was carbon dominated and 2007 with full tungsten PFC's. Parts of the main chamber had been W coated before the 2003 experiments. From spectroscopy no significant change of the carbon content during the plasma operation was observed, which was interpreted as a result of the manifold recycling of C [4].

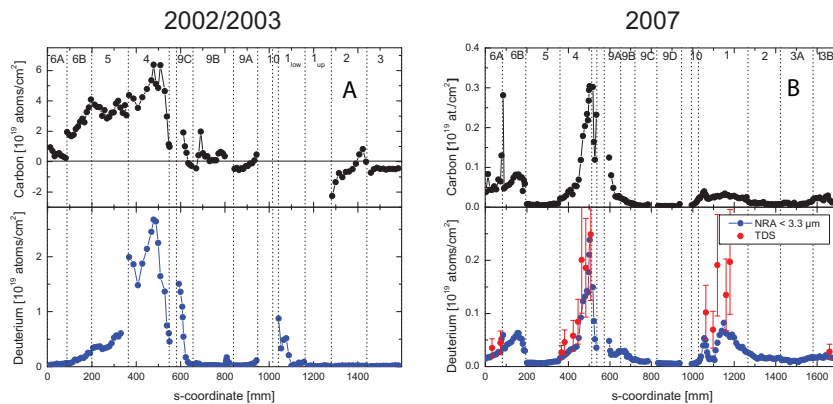


FIG. 2: C and D Deposition on the divertor tiles for C (A) and W (B). Note the different scales for C and W campaigns. Negative numbers are net erosion.

deposition is found as a:CD layers at the inner divertor. The magnetically determined inner strike point was always located at tile 4. Here up to $6 \times 10^{19} \text{at/cm}^2$ carbon are found. Almost the same carbon deposition is on tile 5, decreasing to $5 \times 10^{18} \text{at/cm}^2$ at the baffle region (tile 6A). At the strike point module 4 the deposits form typical a:CD layers with $D/C \approx 0.4$. At the other inner divertor tiles a low D content ($D/C \approx 0.1$) is observed. The jump of the D content from tile 4 to tile 5 correspond with the different divertor materials used. For historical reasons tile 4 was made out of CFC. Laboratory [6] investigations show that the D content of these layers depends strongly on the temperature of the substrate. So the higher D content of tile 4 can be contributed to the lower temperature or, more plausible, on the porosity of the CFC. At the private flux region (tiles 9 and 10) deposition is found close to the strike point region, indicating re-erosion and re-deposition as discussed below for the remote areas. The marker stripes at the outer divertor strike point module (tiles 1) were destroyed, so no carbon deposition and erosion could be determined. On tiles 2 and 3 carbon erosion was found. In general the deuterium content of the outer divertor is low, confirming that this region is erosion dominated. The only deposition is in the shadow region of tile 2, where the upper edge of this tile is shadowed by tile 3 for edge protection. Summing up all tiles a D inventory of $1.48 \sim 2.14 \text{ g}$ is found for the 2002/03 campaign.

The same measurement is shown for the 2007 campaign in *FIG. 2B*, which is scaled by a factor of about 10. Carbon deposition is found at the inner baffle region, the private flux region and to a minor fraction at the outer divertor strike point module. The deposition at the outer divertor

The C- and D-deposition during the 2002/03 campaign is shown in *FIG. 2A* [5]. The results are plotted versus the s-coordinate, which starts at the inner divertor baffle via the private flux region to the outer divertor baffle. The numbering of the tiles is indicated at *FIG. 1*. Dominating

reflects the surface roughness of the VPS coatings used. Spectroscopy yield the C content of the SOL. Comparing the C and W device the C deposition at the inner divertor drops by a factor of 15. In a naive point of view one would expect the carbon content in the SOL to behave similar, but only a reduction by a factor of 2 was found ([8]). Deuterium is deposited at the inner divertor and private flux region as a:CD layers ($D/C \approx 0.4 - 1.0$), similar as after the 2002/03 campaign. TDS measurements confirm this results at the inner divertor, whereas a higher retention at the outer divertor is observed. This yield to implantation of D inside the VPS coatings [5]. From Laboratory investigations it is known that the VPS layers used in AUG show a higher implantation rate than massive tungsten. Possible carbon sources are electrical arcs, remnants from former campaigns, or erosion by oxygen atoms. Consequently the PFCs had been additionally cleaned for the 2008 campaign. In total $0.13 \sim 0.20 \text{ g D}$ are found at the divertor tiles.

3. Deposition at remote areas

As remote areas we subsumimize the areas below and behind the divertor tiles as well as the structures. In AUG layers are found primarily below the roof baffle, indicated as *Re* in *FIG. 1*. For safety purposes the D inventories of de-

posits at remote areas are critically, as they form deuterium rich a:CD layers ($D/C = 0.4 \sim 1$) and a cleaning is hindered by difficult access and the complicated structure. Small Si wafers mounted at these different positions are used as probes for ion beam analysis. Additionally cavity probes, which allow to determine the effective sticking probability of the layer preceeding precursors [6] and quartz micro balance monitors, which give shot resolved information on the layer growth are used [7]. From cavity probes and the decay length of the layer thickness it is deduced that the deposits are formed by activated precursors, which have a high sticking probability. Geometrical reconstruction from cavity probes yields the source of the precursors close to the strike point position.

The amount of D deposited at the divertor region normalized to the total amount of D puffed during discharges is summarized in *Table 1*. During the campaign 2002/03 2.6 % of the D puffed during plasma discharges was found at the divertor. About 60 % of the D deposition is located at the inner divertor, 30 % at the remote areas. For the full tungsten device in 2007 only 0.6 % of the D input was found. A significant part of the D is implanted in the outer divertor VPS layers, as mentioned above. Again about half of the deposition at inner divertor tiles is found at remote areas.

The deposition at the target plates, derived from *Fig 2*, and remote areas is plotted in *Fig 3*. At the inner divertor (*Fig 3B*) the strongest deposits are found at the target plates. Here the layers are eroded again leading to deposits at the remote areas. As the source are the strike point modules an exponential decay toward the remote areas is expected, as observed. For the 2007 campaign the deposition at the target plates are reduced by a factor of

year	Total	inner	outer	remote
2002/03	2.6 %	1.6 %	0.2 %	0.8 %
2007	0.6 %	0.2 %	0.4 %	0.1 %

Table 1: D inventory normalized to the D input found at the inner and outer divertor PFC and remote areas.

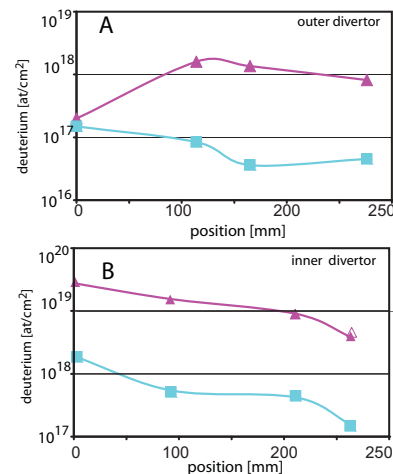


FIG. 3: D deposition below the divertor plotted on the distance from the divertor plates. In magenta the 2003 results in cyan the 2007 results.

20, the deposition is reduced by the same amount, the shape curve is not changed. At the outer divertor the behaviour is more complicated. The re-erosion by the parasitic plasma [7] was taken into account by the selection of the probes position. For the 2003 campaign the deposits at the remote areas are an order of magnitude thicker than at the target plate. The deposits at the target plates are obviously mostly re-eroded again during plasma operation. As the erosion at remote areas was negligible, the deposits could be thicker than at the source, the strike point module. During the W campaign a normal decay from the target plate is observed. This can be explained by the fact that the carbon deposition at the strike point was too low to build up layers, which could be re-eroded.

4. Gas Balance measurements

The standard conditioning of present fusion devices include a wall coating as boronisation to introduce an additional getter material in the main chamber. Before the 2008 campaign the PFC were completely cleaned from former layers. For the start of this campaign no wall coating was used. As initial conditioning only baking and HeGD are used. After this, plasma operation was started for further conditioning. After about 100 shots of plasma operation no out gasing was found anymore. For the gas balance with W wall we restrict our data base to this phase, before the first boronisation of the 2008 campaign. The low amount of boron was confirmed by spectroscopy, which found that boron was below the detection limit during this phase [8].

To obtain accurate balances the gas inlet and pumping systems of AUG has been re-calibrated with respect to a calibrated Baratron [9]. To extent the pressure range, a hot cathode ionization gauge is calibrated for each shot versus a baratron. For the balance particle input by various gas inlet valves Φ_{valves} and the NBI boxes Φ_{Beam} have been taken into account. For the pumping the cryo pump Φ_{CP} , Turbo pumps Φ_{TMP} and NBI boxes Φ_{NBI} are considered. As all pumping systems installed at AUG are limited by conductance, a pressure dependence of the pumping speeds was taken into account. Additionally, the in-vessel cryo pumping speed was determined statically by measuring the amount of gas released after regeneration into the vessel.

The gas flux is derived from the product of the pumping speed and the pressure measured. Test runs with high gas flux and without plasma yield a total accuracy better than 1%. This low value could be not reproduced after plasma discharges. The gas temperature was identified as the dominate error. During experimental days the LN_2 shielding of the in-vessel cryo pump is always kept cold. On other areas and limiters at the main chamber temperatures up to 400K even 10 min after a high power discharge are observed. Even higher temperatures are expected for some shielding of diagnostics, which are intentionally build with poor thermal contact to prevent a heating of the diagnostic parts.

Semi-detached H-mode discharges are foreseen to be the most relevant for ITER, so we concentrate on high density discharges for the gas balance investigations. In AUG a standard H-mode discharge, which is performed on each experimental day, can be used as a basis for gas balances.

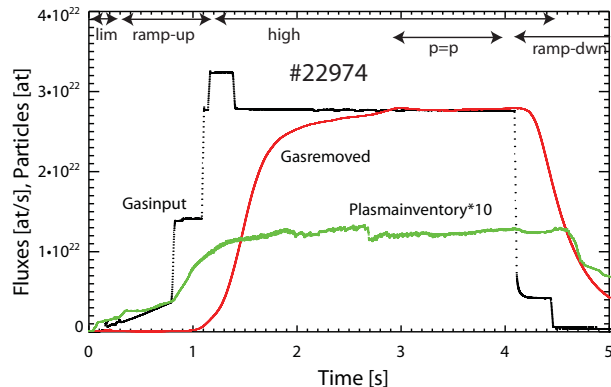


FIG. 4: Gas input and removed gas for a standard H-mode shot. The different phases of the discharges, as used in table 2 are indicated.

This 1 MA shot is heated with 5 MW of NBI, reaches line averaged densities of $9 \cdot 10^{19} m^{-3}$ ($\approx 0.7n_{gw}$) and total gas puff of $1 \cdot 10^{23} at$ during 6 s.

$$R_D = \left(\int (\Phi_{CP} + \Phi_{TMP} + \Phi_{NBI}) dt + N_{pl} + N_{nt} \right) / \int (\Phi_{valves} + \Phi_{Beam}) dt \quad (1)$$

The gas balance for a typical shot of the series of standard shots is shown in FIG. 4. The gas input is the sum of the puffed gas Φ_{valves} and NBI flux Φ_{Beam} . For the

Phase	T_{start}	T_{end}	N_{in}	N_{out}	ΔN_{pl}	R_D
	s	s	$10^{20} at$	$10^{20} at$	$10^{20} at$	
limiter	0.0	0.3	2.2	0.7	2.2	1.35
ramp-up	0.3	1.2	60	1.1	7.2	0.14
high dense	1.2	4.1	799	690	2.5	0.87
p=p	2.9	4.0	339	340	0.6	1.01
ramp-dwn	4.1	6.5	19	164	-0.7	8.05
shot	0.35	6.2	915	869	-	0.95
short term	-5	15.5	947	932	-	0.98

Table 2: Gas balance for the different phases of the standard H-mode shot 22974.

gas removed the flux to the pumping systems is summed up. The plasma inventory N_{pl} is derived from the line averaged density and the plasma volume. Note that the plasma inventory is more than one order of magnitude less than the pumped gas. The discharge can be divided into different phases. The plasma starts as a limiter discharge (lim). Only a minor gas puff of $6 \cdot 10^{20} at/s$ is applied, outgasing of the wall is dominant. For plasma density ramp up (ramp) the puffing is increased up to $3.3 \cdot 10^{22} at/s$. During this phase deuterium is mostly absorbed by the wall. After the high density phase is reached (high), the plasma content is constant. The neutral pressure at the divertor is rising on a longer time scale, reaching steady state conditions at 2.9 s (p=p). As the gas input is reduced (4.1 s), strong outgasing starts (ramp-dwn).

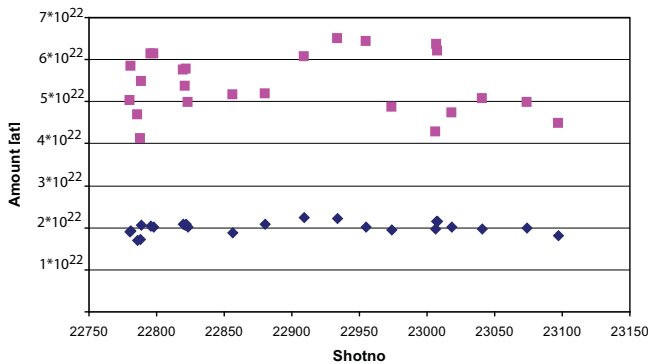


FIG. 5: Gas input needed to reach the steady state phase. The magenta points show the amount of gas puffed, the blue the retained gas.

influence on the whole discharge gas balance. During ramp-up the wall is loaded, leading to a low value of R_D . The high density phase shows an almost balanced gas input and output. These quantities are balanced during the steady state phase. To compare shots with different densities, which may not reach steady state conditions, the shot integrated values are needed. The outgasing is discussed below.

The standard H-mode discharge is performed on each experimental day, which gives a data base of 30 discharges obtained for unboronized wall conditions during the 2008 campaign.

To qualify the wall retention the ratio R_D is defined in Eq.1. Additionally the neutral gas N_{nt} is taken into account. The gas fluxes during the different phases are summed up to calculate R_D as shown in table 2. Additionally the data for the whole plasma discharge, i.e. the time slice with plasma current $I_p \geq 200kA$ and the 15 s after the discharge (short term) are added. The fraction R_D indicates outgasing for the limiter phase. As the total amount of gas is low, this has almost no influence

Small variations on the standard shots indicated the use of this shot for piggy back programs. Averaging these discharges leads to a retention of $1 - R_D = 8.2 \pm 3.3 \%$ for the whole discharge and $1 - R_D = 1.5 \pm 3.5 \%$ for the steady state phase. The statistical error of 3 % agrees with the expected uncertainty due to the gas temperature.

To reach the steady state phase it is necessary to saturate the wall. Wall saturation requires high gas puffing rates, and is only reached for high density shots. The amount of gas needed to fill up the wall is shown in FIG. 5. Typical $4.1 \sim 6.5 \times 10^{22}$ at of D are needed to be puffed to reach the steady state phase ($p=p$). The variation of this value is caused by different plasma conditions as for example strike point position. Calculating the gas retained in the wall $19 \pm 1 \times 10^{21}$ at D is found. Note that this value show much less variation than the amount of gas puffed. This hints that the wall loading is almost independent on details of the discharge. The gas retained is equal to 44 monolayers D on the PFCs. Here we take the geometrical surface of torus as effective area.

The retention ratio R_D taken for the whole plasma discharge (shot) for all plasma discharges during the 2008 campaign after initial conditioning and before the first boronisation are plotted in . The first finding is that no discharge with $R_D > 1$ are found, i.e. even for high heating powers no significant outgasing from the wall is observed. After boronisation shots with gas release are observed again, as in many other devices. These points to the storage of D in the boron layers. For low gas fluences a strong increase of R_D is found. For higher fluencies the R_D approaches asymptotically the $R_D = 1$ line. As the whole shot is used for this evaluation, the retention is always larger than for steady state phase. For high gas puff very low retention of D is found.

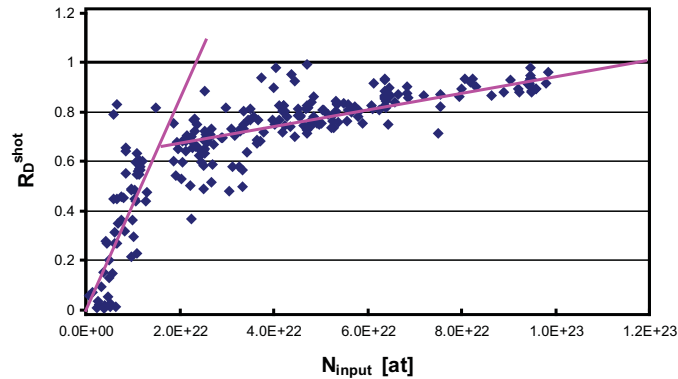


FIG. 6: R_D^{shot} for all discharges of the 2008 campaign after initial conditioning and before the boronisation.

5. Gas Balance with carbon wall

Gas balances with carbon wall were reported in [10]. In the view of the new calibration the data have been re-evaluated. The absolute values differ by less than 10 %, confirming the former results. Unfortunately the new calibration is not completely valid for the older data, as parts of the gas inlet system and the outer divertor had been changed in between. During the carbon phase AUG was always operated with boronised PFC. A plot similar to FIG. 6 shows, especially for low density, strongly heated scenarios significant outgasing from the wall. We sup-

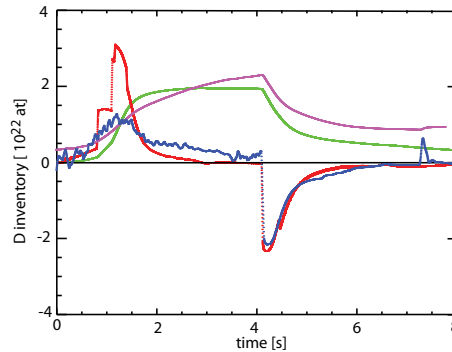


FIG. 7: Comparison of the gas balances for carbon (# 17308) and tungsten wall (# 22974). The difference of gas puff and removal is shown in red (W) and cyan (C). The integral in green (W) and blue (C).

pose that this behavior is mostly due to the boron layers, as a similar behaviour is observed for boronized W wall. To the knowledge of the authors no data for pure carbon PFC exists. Even if no boronization was applied, boron layers of some micron thickness remain from former campaigns [11].

FIG. 7 shows the comparison of two similar high dense discharges with carbon and tungsten PFCs. The balance, defined by the difference of the puffed and pumped gas, for a tungsten discharge is shown in red for carbon in cyan. The abscissa is shifted slightly so, that the ramp down phase of both discharges overlay. The different phases and the wall loading are similar for carbon and tungsten PFCs. The ramp up scenario for the discharges is very different, but for both a wall inventory is build up. For the tungsten PFC a phase with no additional wall loading is reached from 4.2 till 5.4 s. For carbon a strong reduction of the puffed gas is also observed, as the control systems needed less gas to maintain the density. But a significant amount of gas is always retained. Typically $5 \times 10^{21} \text{at/s}$ are retained during this phase. During the ramp down both discharges show very similar behaviour.

6. Long Term Retention

In general, measurement of long term outgasing is hindered by the operation scheme of AUG. As the inventory of the in-vessel cryopump is restricted by safety reasons, regeneration is needed after each high density shot. Due to this the outgasing could be only determined for typically 100 s. One example with a delayed regeneration after a high density discharge is shown in FIG. 8. The data gap at 45 s is due to the closing of the NBI valves, which changes the pumping speed. A base vacuum of $2.7 \times 10^{-7} \text{mbar}$ equal to a pumped flux of $4 \times 10^{18} \text{at/s}$, as measured before the shot, was subtracted. The curve shows an exponential decay after 400 s with a time constant of 138 s. The first part has a time constant of about 22 s. Integrating the curve, the fraction of long term outgasing could be measured. The results for similar shots (1 MA, $\approx 7.3 \text{ MW}$ auxiliary heating, $n_e \approx 1 \times 10^{20} \text{m}^3$) with W and C PFCs are compiled in the table 3. The total puffing rate for both shots is similar. As mentioned above a higher fraction is pumped for W wall during plasma operation. Outgasing of the wall starts during the shot, as the gas puffing rate is reduced during plasma ramp down to avoid density disruption limit. During this phase more gas is pumped for the tungsten wall, reflecting the faster outgasing. The next time slice is defined by the fast data acquisition system, which records data until 15.5 s. The long term outgasing phase is monitored until 650 s. In total 3% more gas is pumped for this shot than puffed, i.e. the balance is closed within the error bars. Most of the puffed gas is pumped during the plasma operation. The strongest outgasing occurs as the plasma is ramped down. Only about 10% is remaining in the vessel as the plasma current ends. The fast decay rate of 20 s right after the discharge leads to a removal of most of the gas within some minutes. Probe data, as mentioned above found a deposition of 0.6% of the puffed gas for the 2007 campaign. Both methods agree within the error bars. The low D wall inventory is confirmed by the fact that, in contrast to the C wall, no GD cleaning is needed in AUG for normal plasma operation anymore.

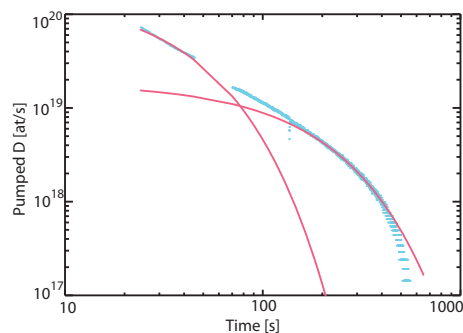


FIG. 8: Gas removed after a discharge with W PFCs. Exponential functions are fitted to the tile slice 25-40s and 200-400s.

For carbon PFCS a significant amount of D is missing. The long term outgasing was not measured as it was covered by an automatically started HeGD. Former investigations yield that about 20 % of the puffed gas was released as hydrocarbons during HeGD and on a day time scale [10]. This value is an average on different shot scenarios and has a bigger error bar. Again a good agreement of the long term retention and the measurements by probes (2.4 %) is found.

	22974		17308	
Phase	$10^{20} at$	%	$10^{20} at$	%
Total Puff	947		907	
Total Pumping	973	103	782	81
Normal Plasma	692	73	578	64
ramp down	164	17	114	13
Pumping 15 s	76	8	49	5
Pump long term	41	4	?	?
Probes found		0.6		2.7

Table 3: Long Term Retention for W (#22974) and C (#17398) PFC's.

7. Extrapolation to long term discharges

Gas balances are used to establish the technique needed during the H and D phase of ITER, to evaluate an operation scheme with low permanent wall retention and to extrapolate to ITER. Whereas the probe technique yields an average on all kinds of discharges the gas balance can be used to investigate different discharge scenarios. We assume that the typical operation of ITER will be at high gas fluxes. So the wall saturation regime will be reached. Assuming the same behavior as in AUG and a 10 times bigger geometrical surface, an inventory of 0.5g T is expected for wall saturation. After wall saturation a steady state phase will occur. However, the increase of the additional inventory cannot be extrapolated from the ASDEX Upgrade results because the wall temperatures in ITER will be much higher and the measurement errors of the gas balance in AUG - although already quite small - are still too large.

References

- [1] Neu, R. et al., "Final steps to an all tungsten divertor tokamak", J. Nucl. Mat, **363-365**, (2007), 52.
- [2] Neu, R. et al., "Plasma wall interaction and its implications in an all tungsten divertor tokamak", PFC, **49**, (2007), B59.
- [3] Mayer, M. et al., "The Deuterium Inventory in ASDEX Upgrade", Nucl. Fusion, **47** (2007) 1607.
- [4] Kallenbach, A. et al., "Spectroscopic investigation of carbon migration with tungsten walls in ASDEX Upgrade", J. Nucl. Mat, **363-365**, (2007), 60.
- [5] Mayer, M. et al. "Carbon balance and deuterium inventory from carbon dominated to a full tungsten ASDEX Upgrade", J. Nucl. Mat, (PSI18), accepted for publication, (2008).
- [6] Mayer, M. et al., "Further inside into the mechanism of hydrocarbon layer formation below the divertor of ASDEX Upgrade", Nucl.Fusion, **46**, (2006), 914.
- [7] Rohde, V. et al., "Carbon erosion and a:C-H layer formation ", J. Nucl. Mat, **337-339**, (2005), 104.
- [8] Kallenbach, A. et al., "Non-Boronized operation of ASDEX Upgrade with full-tungsten plasma facing components", these proceedings.
- [9] Rohde, V. et al., "Gas balance in ASDEX Upgrade with tungsten wall", J. Nucl. Mat, (PSI18), accepted for publication, (2008).
- [10] Mertens, V. et al., "Hydrogen Gas balance in ASDEX Upgrade with divertor II b", ECA **27A** (2003) P-1,128.
- [11] West, W. P. et al., "Plasma Operation and Monitoring of Wall Conditions on DIII-D Over Extended Periods Between Boronizations", J. Nucl. Mat, (PSI18), accepted for publication, (2008).